Received November 27, 2019, accepted December 15, 2019, date of publication January 15, 2020, date of current version January 29, 2020.

Digital Object Identifier 10.1109/ACCESS.2020.2966752

Illuminance Sensing in Agriculture Applications Based on Infra-Red Short-Range Compact Transmitter Using 0.35um CMOS Active Device

ROMAN SOTNER[1], JAN JERABEK[2], LADISLAV POLAK[1], (Member, IEEE), JIRI PETRZELA[1], WINAI JAIKLA[3], AND SUNTI TUNTRAKOOL[3]

[1]Department of Radio Electronics, SIX Research Center, Brno University of Technology, 61600 Brno, Czech Republic
[2]Department of Telecommunications, SIX Research Center, Brno University of Technology, 61600 Brno, Czech Republic
[3]Department of Engineering Education, Faculty of Industrial Education and Technology, King Mongkut's Institute of Technology Ladkrabang, Bangkok 10520, Thailand

Corresponding author: Roman Sotner (sotner@feec.vutbr.cz)

Research described in this paper was financed by Czech Ministry of Education in frame of National Sustainability Program under Grant LO1401. For research, infrastructure of the SIX Center was used.

ABSTRACT This paper introduces a novel electronic system for simplex low-bitrate infra-red (IR) communication applications. The transmitter is implemented completely by analog building blocks, formed with the help of a recently fabricated chip that includes active elements allowing various modular interconnections. For the design of this chip, the ON Semiconductor C035 0.35μm I3T25 technology was chosen due to the trade-off between cost, efficiency and obtainable parameters. The designed transmitter operates as a voltage-to-duty cycle converter, using pulse width modulation that causes ON/OFF keying of the carrier signal for infra-red (IR) diode. The duty cycle variable between 7% and 83% is modulated by the input voltage (in the range of $\pm$0.8 V) of the transmitter. The use case of the proposed concept in the measurement of illuminance within the range of 30 lx and 550 lx is also presented. The quality of the transmission was evaluated as the error between the transmitted and received values of the duty cycle (kept mostly below 10 %). The maximal power consumption of the transmitter reaches 180 mW.

INDEX TERMS Generator, illuminance sensing, IR transmitter, modular CMOS design, photoresistor.

I. INTRODUCTION

In the field of satellite [1], optical [2] and terrestrial communication systems [2]–[4], achieving a reliable connection over long distances and overcoming high signal attenuation are among the main requirements in the planning of these wireless communication links. Such systems can be complex and expensive. Research in the field of remote signal sensing focuses mainly on signal processing [5], automation and optimization of the measurement [6] rather than on hardware and circuit design [7]. High amount of transferred data and high bitrates (Mbps, Gbps) are quite common for these systems. Depending on the particular system (e.g. satellite, mobile, optical), the power required for the transmitter can reach very high values leading to substantial high power consumption (from tens to hundreds of Watts or even more) [1]–[4]. However, in small areas and closed environments, simpler solutions can be applied.

The associate editor coordinating the review of this manuscript and approving it for publication was Mohsin Jamil.

In such use cases, a short distance communication link with low bitrate (kbps) as well as low power consumption (less than 1 W) is sufficient and it is usually a better solution than the standard discrete one (usually requiring more than 1 W).

Short-range infra-red (IR) communication systems [8] can utilize various modulation techniques [9]–[11]. Digital pulse interval modulation (DPIM) is one of the most frequently used modulations for optical communications [12]. However, the IR technology does not serve only communication purposes. Also biomedical applications are well known, non-invasive glucose monitoring, for instance [13].

In this paper, the design of a simple circuitry optimized for sensing and remote transmission of information about the illuminance (with value represented in hundreds of lux [14]) for indoor use cases is presented. Its usage in the field of small-area agriculture and vegetation observation is considered.

Of course, many plants require natural sunlight for their healthy growth and, therefore, monitoring and/or control systems are required for indoor scenarios. However, different

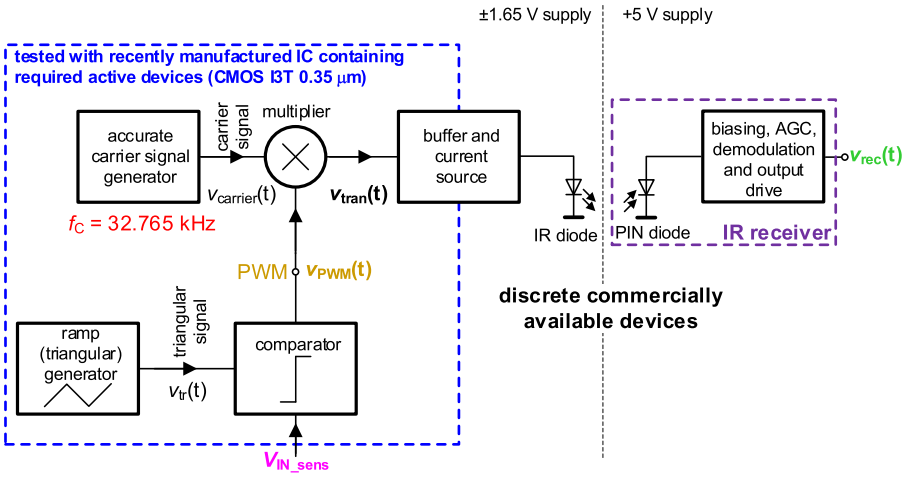

FIGURE 1. Block topology of the IR communication system and signal processing from sensors (including transmitter and receiver).

plants require different amount of sunlight with different intensity in order to grow optimally [15]. Therefore, it is useful to measure and control this quantity, especially for high quality cultivation of plants, for instance in aquariums or in case of any kind of shading system in general. Information about the intensity of light (in the form of illuminance derived from the duty cycle in studied case) can be transmitted to any place in near neighborhood. Some aquarium boxes using own source of light may utilize this information also for control purposes. The transmitter can be supplied from the power line used to control the aquarium climate (heating/cooling/humidity). The receiver, based on an IR remote control system, can be designed as a portable box supplied by batteries.

This work targets mainly the design of the electronic circuit suitable to operate as an IR communication system and our goals are as follows:

1) to design a simple system for simplex low-bitrate IR communication based on the pulse width modulation (PWM) [11],
2) to process the sensed signals having amplitude up to ±500 mV correctly. Linear voltage processing is limited due to the very low power supply voltage of the active elements (±1.65 V),
3) to design a compact and simple transmitter using recently introduced CMOS integrated building blocks [16] because of its low complexity and power consumption and,
4) to realize measurements in real environment (plant aquarium in our case) in order to verify functionality of the proposed concept.

The proposed transmitter (later introduced in detail) can be also designed with discrete off-the shelf elements (requiring at least six commercially available IC packages). A comparison of the discrete and the designed solution is presented in Table 1. The number of IC packages, power supply voltage and power consumption are the main differences between our solution and the discrete one.

TABLE 1. Comparison of the features of the discrete and proposed way of construction of the IR transmitter.

	Discrete solution	The designed solution
Number of blocks	5	5
Number of active elements (AEs) required	6	8
Number of IC packages	6 *	2 **
Supply voltage	at least ± 5 V	at least ± 1.65 V
Expected power consumption	units of Watts	low (hundreds of mW)

Notes:
* Commercially available devices
** Two pieces of our IC device and one additional BJT are required

The rest of this paper is organized as follows: Section II introduces the proposed concept of the designed IR communication system and explains principles of all blocks in detail. The complete topology of the transmitter is presented and described in Section III. Experimental results of the verification of the pulse width modulator (a part of the transmitter), and simplex transmission (waveforms in the system and at the receiver side), when trial DC input voltage is used as a replacement of sensed signal, are presented in Section IV. Section V introduces a practical application of the proposed system in case of measurement and transmission of the value of illuminance.

The proposed concept as well as comparison of its features with similar solutions are presented in Section VI. The paper is concluded in Section VII. Appendix supplements this work

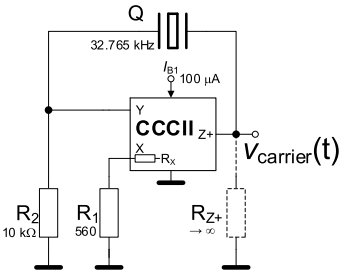

FIGURE 2. Carrier wave generator with accurate repeating frequency of 32.765 kHz.

by a brief explanation of the principles of relevant active elements (AEs) required for the design of the system.

II. PROPOSED TRANSMITTER

Topology of the system forming the IR communication chain is shown in Fig. 1. The system consists of five key parts serving the following purposes: a) accurate carrier signal generator – generation of the carrier voltage $v_{carrier}$ with the stable frequency of 32.765 kHz (f_c), b) ramp (triangular) generator – generation of the ramp (triangular) signal v_{tr} for PWM, c) comparator –providing the result of coincidence of v_{tr} and slowly changing input voltage v_{IN_sens} from various sensor sources (readouts), d) voltage multiplier – multiplication of $v_{carrier}$ and PWM signal $v_{PWM}(t)$. It provides ON/OFF keying based on the width of the modulated PWM wave, to obtain the signal v_{tran} for transmission, and e) voltage buffer and current source – for proper IR diode biasing. Each functional block of the proposed IR communication system will be presented in detail in the following subsections.

The transmitter uses building blocks, which are based on AEs fabricated recently in 0.35 μm I3T25 ON Semiconductor technology. More details about these AEs can be found in [16]. A current controlled current conveyor of second generation (CCCII), two analog multipliers (MLTs) of two differential input voltages providing output product in the form of current (marked as CMOS MLT and BJT MLT) and a voltage differential difference buffer (VDDB) were used. A brief description of the principles of all these AEs is available in Appendix . Outputs from real measurements of individual parts and also from the whole system can be found in Sections III and IV, respectively.

A. ACCURATE QUARTZ-BASED GENERATOR PROVIDING CARRIER WAVE SIGNAL

In order to achieve a proper light transmission at the expected wavelength of 940 nm, the TSAL6100 [17] IR diode with the bias current alternating with the repeating frequency of 32.765 kHz was used. Very stable and accurate carrier frequency is required by the chosen type of the IR remote receiver (TSOP1733 [18]) because its sensitivity is the highest at this particular frequency. The circuitry of the carrier signal generator (see Fig. 2) employs a quartz (with $f_{carrier}$ =

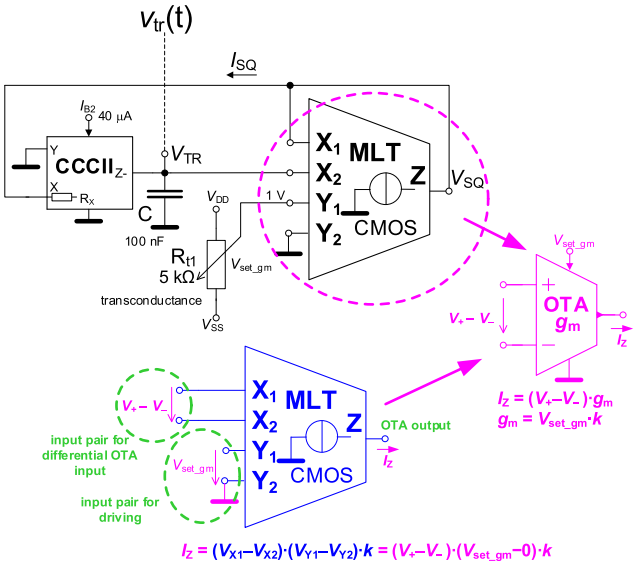

FIGURE 3. Adjustable ramp (triangular) wave generator based on CCCII and MLT AEs.

32.765 kHz) and a CCCII element in order to realize the voltage-limiting amplifier having saturated output. The value of the resistance visible at the Z+ terminal is theoretically going to infinity ($R_{Z+} \rightarrow \infty$). Therefore, the overall theoretical gain of the loop is $R_{Z+}/R_1 \rightarrow \infty$. The bias current of the CCCII ($I_{B1} = 100\ \mu A$) is set to reach a tradeoff between request of low value of the internal resistance of the X terminal $R_X \cong 500\ \Omega$ [16] and the expected power consumption. The quartz is connected between the Z+ output terminal and the Y voltage input together with the grounded R_2 resistor in order to create an equivalent of RLC frequency selective feedback. This positive feedback leads to square wave oscillations. The stability of the frequency is preferred over other features of this block (there is no need for an exact shape of the generated waveform).

B. RAMP GENERATOR FOR PWM MODULATOR

A completely resistor-less generator of ramp (triangular) signal for PWM modulation uses a very simple connection of CCCII and MLT active elements (see Fig. 3). CCCII was used to create an integrator providing control of its time constant by adjusting the R_X (I_B current) and the Schmitt trigger by a simple OTA element (widely used in many standard solutions [19]). The threshold voltage level of this trigger is defined as:

$$V_{TR} = V_{SQ}\left[\frac{g_m R_X - 1}{g_m R_X}\right], \tag{1}$$

where V_{TR} and V_{SQ} are the amplitudes of the triangular and square waves, respectively. The change of the voltage across the capacitor C can be expressed as:

$$\Delta v_C = v_C(t = T/2) - v_C(t = 0) = \frac{I_{C\,max}}{C}\frac{T_{ramp}}{2}, \tag{2}$$

where $\Delta v_C = 2V_{TR}$ is the change of the voltage in the half-period of the triangular wave, and I_{Cmax} is given by I_{B2} and

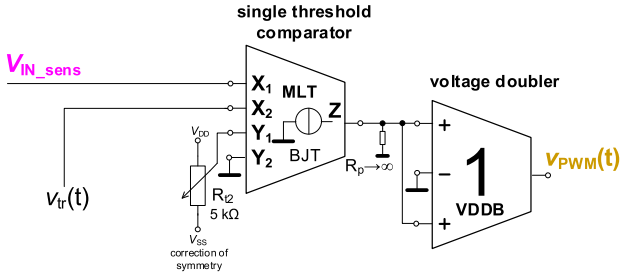

FIGURE 4. Comparator for PWM generation using MLT and VDDB AEs.

the current gain of the internal CMOS mirror [16] as: $I_{C\max} = 10 \cdot I_{B2}$. After substitution and rearrangements of previous expressions, the ideal form of the repeating frequency of this ramp generator can be expressed as:

$$f_{ramp} = \frac{I_{C\,\max}}{4C \cdot V_{TR}} \cong \frac{10 \cdot I_{B2}}{4C \cdot V_{SQ}} \left(\frac{g_m R_X}{g_m R_X - 1} \right). \qquad (3)$$

C. COMPARATOR FOR PWM MODULATOR

The comparator of the PWM modulator (see Fig. 4) includes BJT MLT, which has the transconductance set to a very low but nonzero value in order to cancel the DC offset and the asymmetry of the pair of voltage inputs X_1, X_2. Theoretically, this controlled current source has an infinite output resistance ($R_p \to \infty$) without load. Thereby, the output level automatically reaches saturation (almost ±1.65 V) even for small value of g_m (operation of the MLT is identical as in Fig. 3). When the output voltage is outside the range of ±500 mV, nonlinearity of the OTA (i.e. MLT) causes slight slope degradation. Therefore, in studied case, the design of linearly operating system assumes limits of ± 500 mV. In order to improve the quality of the shape of generated square wave, an additional voltage buffer-doubler based on VDDB is added (see Fig. 4). It brings a faster reaction to the input changes (there is an improved shape of the edge of rise time and fall time due to the "gain" = 2). The change of the output state (v_{PWM}) occurs when V_{IN_sens} and v_{tr} are equal. It is clear that V_{IN_sens} provides the setting of the threshold. The limit of the threshold voltage (V_{IN_sens}) was found as ±1 V and it is given by the features of the MLT element [16].

D. MULTIPLICATION OF CARRIER WAVE AND PWM SIGNAL

The core of this part, depicted in Fig. 5, is quite simple. A single multiplier ensures multiplication of the carrier and PWM signals as well as the DC level shifting in order to obtain required polarity and also duty cycle control. The V_{Y2} is set to +1.65 V (V_{DD}), therefore, v_{tran} is generated only when v_{PWM} reaches negative polarity. Otherwise, the v_{tran} voltage is close to zero. This setting must be applied for the proper signal processing in the TSOP1733 receiver, where GND (0 V) in TTL represents the active level. The receiver

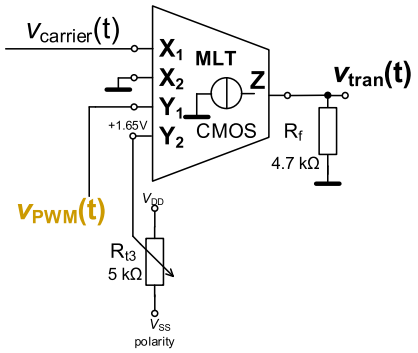

FIGURE 5. Multiplier for ON/OFF keying based on MLT active element.

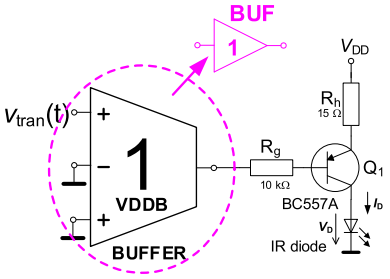

FIGURE 6. Output drive with buffer employing VDDB and current source/switch.

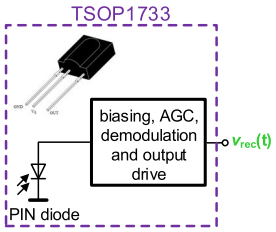

FIGURE 7. The TSOP1733 IR receiver module.

continuously provides +5 V output when there is no input signal (in expected range of wavelengths).

E. BUFFER AND CURRENT SOURCE

This block ensures the conversion of the signal produced by forthcoming blocks in order to source the IR diode (current driving). The voltage buffer can be implemented by the VDDB device (see Fig. 6). The current source operates as a BJT switch (with PNP BC557A BJT transistor [20]) controlled from the buffer and supplied from the source providing +1.65 V (V_{DD}). Resistors R_g and R_h are set properly in order to protect the BJT and the buffer outputs, and to limit the maximal drain current.

F. IR RECEIVER

The well-known compact TSOP1733 IR receiver [18] is optimized for the wavelength of 940 nm and integrates all important blocks for the signal processing in a single package (see Fig. 7).

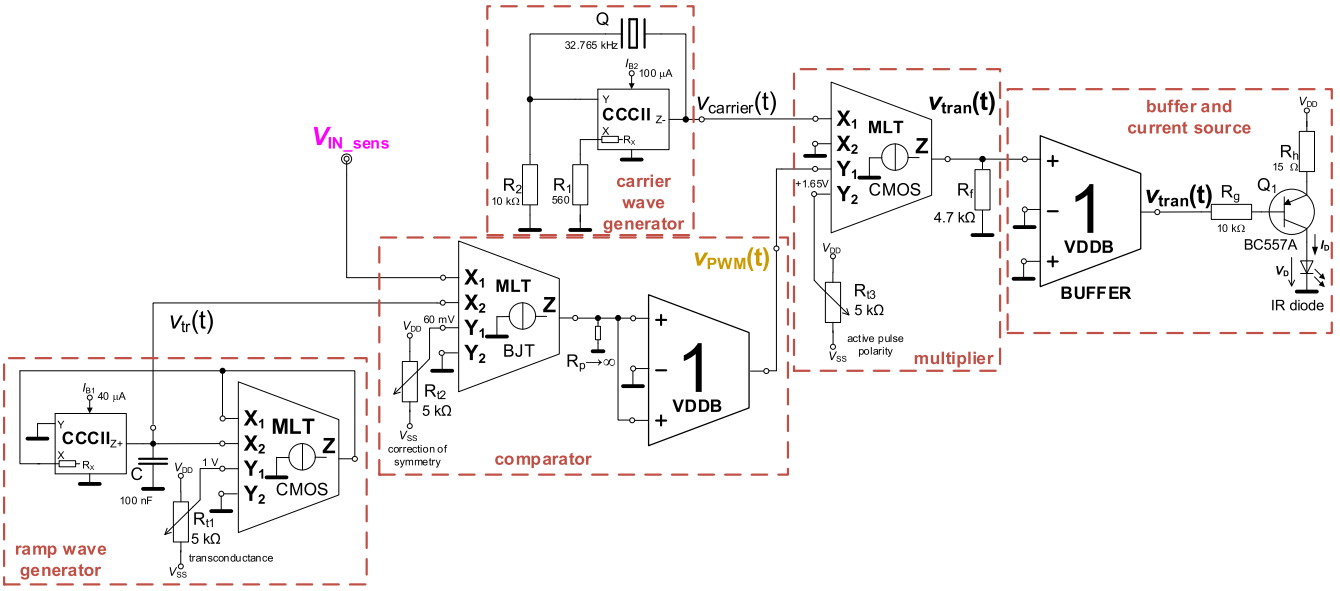

FIGURE 8. The complete topology of the proposed IR transmitter with AEs from IC chip [16], requiring only several passive components and one discrete BJT transistor.

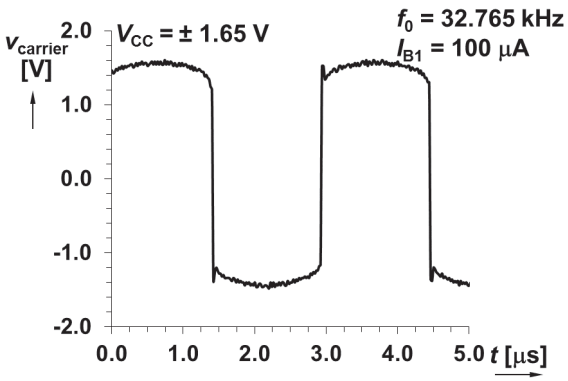

FIGURE 9. An example of the carrier waveform (measurement).

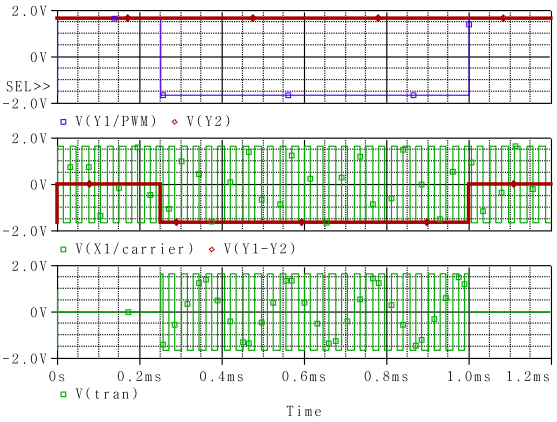

FIGURE 10. Illustration of the signal processing for transmission in the "multiplier" block (ideal blocks).

The output terminal provides TTL (+5 V or 0 V) with the zero level considered as active. The TSOP1733 belongs to the family of miniaturized receivers of IR remote control systems using PCM modulation [10]. It supports very slow data communication (data rates up to 2.4 kbps) sufficient for studied case. In this receiver, the photodiode with a large and neutrally doped intrinsic region (PIN) serves as the photosensor.

III. COMPLETE TOPOLOGY OF THE TRANSMITTER

The complete circuitry of the proposed IR transmitter is shown in Fig. 8. The design specifications are as follows. The carrier wave ($f_{carrier}$) of 32.765 kHz is given by a quartz (Q) oscillator, important for proper functionality of the IR receiver. This passive element directly determines the $f_{carrier}$ having a very stable value that is almost independent of external influences (temperature, supply voltage fluctuations, etc.). An example of the generated carrier waveform is depicted in Fig. 9.

The ramp wave generator uses a simple circuitry without special demands on the accuracy of the repeating frequency. Thereby, the standard approach using charging of a capacitor (with $C = 100$ nF) is sufficient. In the Schmitt trigger part of the circuitry (see Fig. 8), the transconductance of the operational transconductance amplifier (OTA) has the value of $g_m \cong 1.3$ mS obtained by $V_{set\_gm} = 1$ V. The bias current I_{B2} serves for the adjustment of the repeating frequency between 120 Hz and 1.76 kHz (obtained by $I_B = 5\ \mu\text{A} \rightarrow 50\ \mu$A). Note that the frequency of the modulation signal (f_{PWM}) must be several-times lower than the $f_{carrier}$. Therefore, the design of the ramp generator operating in hundreds of Hz is intentional. When V_{SQ} reaching almost the saturation level is considered ($v_{sq} \cong 1.65$ V

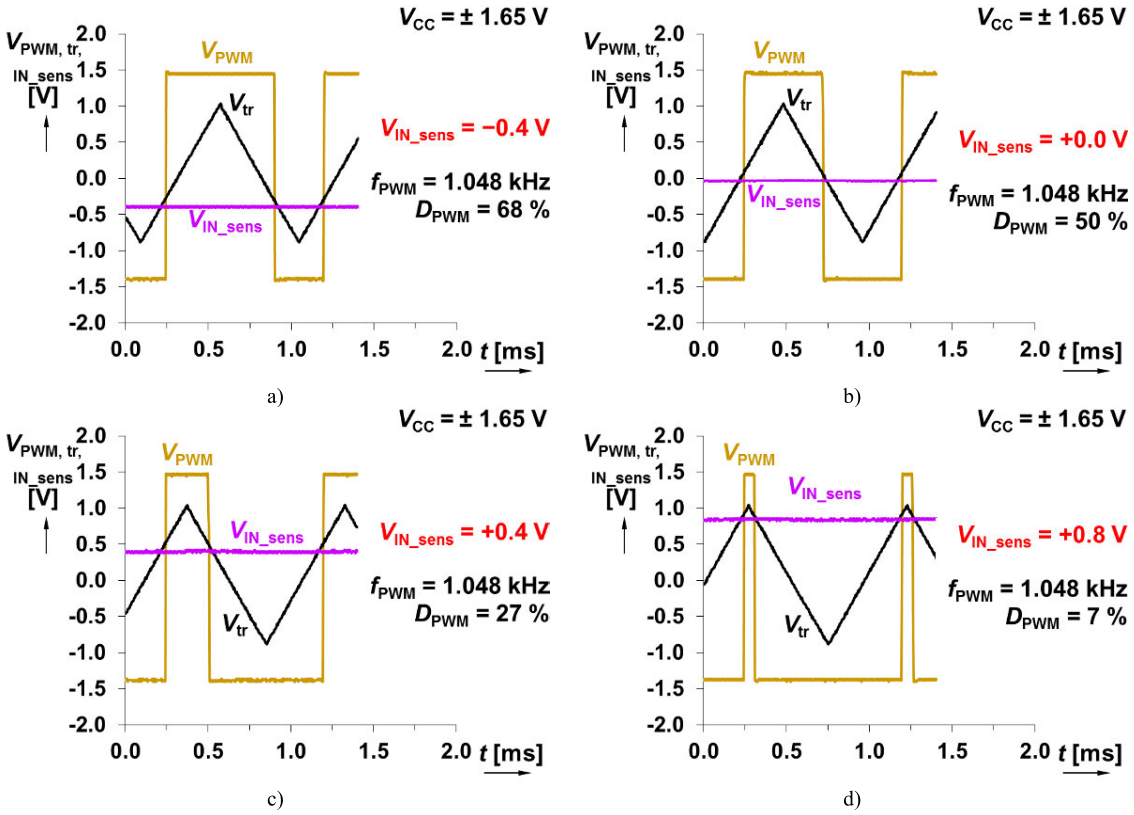

FIGURE 11. Experimentally tested generation of voltage v_{PWM} while setting: a) D_{PWM} = 68%, b) D_{PWM} = 50%, c) D_{PWM} = 27% and d) D_{PWM} = 7%.

and $V_{TR}/V_{SQ} \approx 2/3$) and $f_{ramp} = 1$ kHz, then I_{B2} calculated from (3) is 44 μA. Note that in the case of real measurement, frequency $f_{ramp} = 1$ kHz was obtained for slightly different bias current ($I_{B2} = 40$ μA).

The design of the comparator without hysteresis for PWM generation is an easy task. The change of the state at output (the voltage gain reaches very high values - $g_m \cdot R_P = g_m \cdot \infty \rightarrow \infty$ in ideal case) occurs when the difference of input voltages is close to zero. The DC voltage of 60 mV was set at the second differential pair of inputs (Y_1, Y_2) in order to achieve a particular small value of g_m as well as for compensation of small asymmetry.

The multiplier block in the core of the transmitter operates very simply. The DC offset of +1.65 V at the input Y_2 of the multiplier shifts the whole result of subtraction to negative polarity only (signal between 0 and −1.65 V). Thereby, the result of the multiplication of the signal at X_1 and the difference between $Y_{1,2}$ inputs, described as $v_{tran} = v_{carrier} \cdot (v_{PWM} - 1.65)$, is represented as the current flowing from the Z output of MLT. This current is transformed to voltage by $R_f = 4.7$ kΩ. This value was selected for transformation of the expected currents in hundreds of μA to voltage drops in hundreds of mV. The illustration of the operation of this block is shown in Fig. 10.

The voltage buffer using the VDDB and the current source using a BJT transistor form the last part (output drive) of the transmitter. Based on the nomogram in [17], for forward diode current $I_D = 10$ mA, the forward voltage V_D reaches approximately 1.2 V. In case of collector currents reaching tens of mA, the saturation voltage of the used BJT BC557 is $V_{CEsat} \cong 0.3$ V as noted in [20]. The output drive branch, including an IR diode, uses an asymmetrical power supply of 0 and +1.65 V. Hence, the value of the resistor in the collector can be calculated as $R_h \cong (V_{DD} - V_D - V_{CEsat})/I_D \cong (1.65 - 1.2 - 0.3)/10 \cdot 10^{-3} \cong 15$ Ω. In the state of transmitting, the value of the static current $I_D \approx 12$ mA was measured.

The CMOS voltage buffer (formed by the VDDB) is not able to supply very low loads in the range of units to tens of Ohms. Therefore, the resistor $R_g = 10$ kΩ in the base of the transistor is used to limit the I_{BASE} current (100 μA). Chosen setting falls into the save operational range of the voltage buffer. Moreover, the base-emitter saturation voltage ($V_{BEsat} = 0.7$ V) [20] and the maximal voltage $v_{tran} = 1.65$ V of the VDDB (positive polarity considered) are also known. Hence, its calculation is very simple: $R_g \cong (V_{DD} - V_{BEsat})/I_{BASE} \cong (1.65 - 0.7)/100 \cdot 10^{-6} \cong 10$ kΩ (values rounded to fabrication series).

IV. EXPERIMENTAL TESTS

Functionality of the proposed circuitry is verified in two steps. First step focuses on the generation of the PWM (i.e. on these modules: ramp wave generator and comparator).

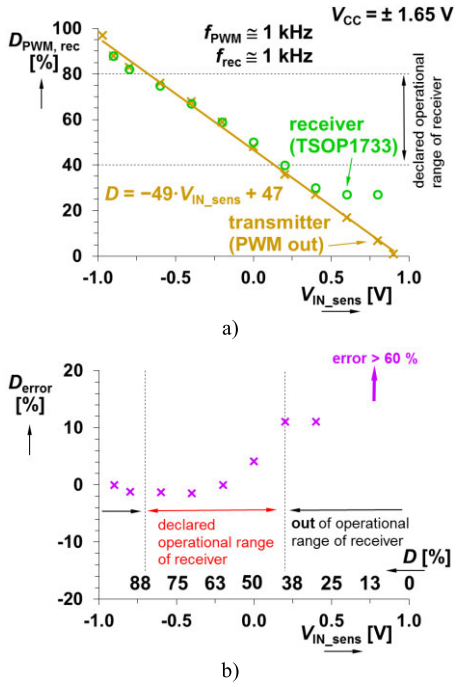

FIGURE 12. Comparison of the duty cycle in the transmitted and received signal (measurement): a) dependence of the transmitted and received duty cycle on V_{IN_sens}, b) error between the transmitted and received duty cycle.

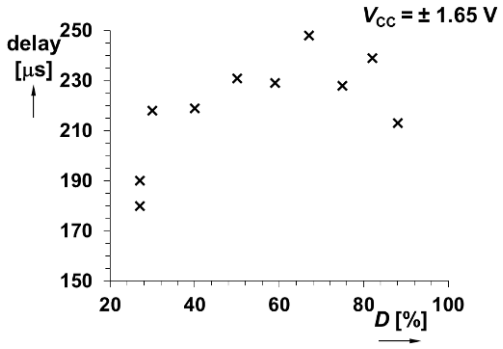

FIGURE 13. Processing delay at the receiver side in dependence on current value of the duty cycle (measurement).

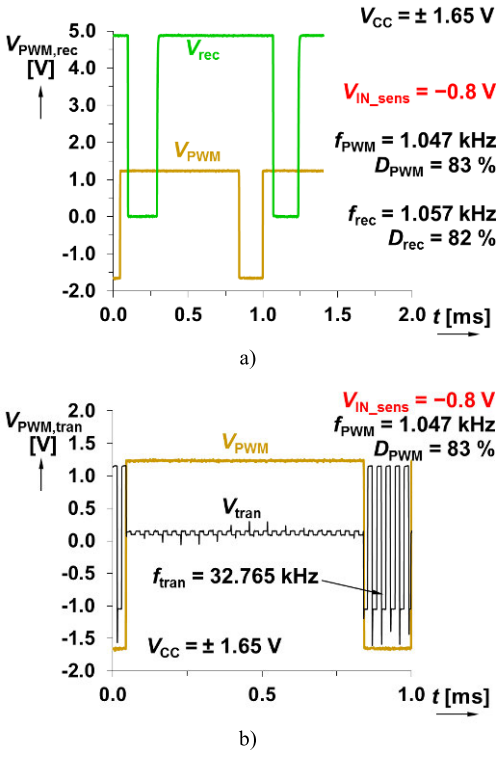

FIGURE 14. Transmission of DC voltage in the form of duty cycle for V_{IN_sens} = −0.8 V (measurement): a) v_{PWM} and v_{rec}, b) v_{PWM} and v_{tran}.

In the second step, attention is given to the analysis of the whole communication chain (transmitter and receiver) when either a simple signal or the real-scenario information is transmitted.

A. PWM GENERATION

The DC voltage was connected to the input terminal V_{INsens} as the source signal. The variation of its value drives the duty cycle of v_{PWM} voltage (D_{PWM}). The supply voltage and dynamic input range of AEs (MTL and VDDB) limit the maximal and minimal values of V_{IN_sens} (theoretically $\pm 1.65/2 \cong \pm 0.8$ V because of the "gain" obtained by the VDDB element of the comparator) as well as available values of D_{PWM}. Figure 11 shows the change of D_{PWM} for several V_{IN_sens} values (particular values of D_{PWM} were: 68, 50, 27 and 7%). The real value of the duty cycle D_{PWM} varies between 83% and 7% for V_{IN_sens} values between ±0.8 V. The maximal range of D_{PWM}(1% → 97%, actually) can be obtained for V_{IN_sens} varied between −0.97 V and +0.90 V (in the case of real measurement). The details about dependence of D_{PWM} on V_{IN_sens} are shown in the next section.

B. WHOLE CHAIN: TRANSMITTING AND RECEIVING

The complete communication chain (see Fig. 1) was tested by lab measurements. The operating range of V_{IN_sens} between −1 V and +1 V was found (slightly higher than the expected range of ±0.8 V). However, the TSOP1733 IR receiver has limited reaction on the duty cycle variation (approximately from 40% up to 80%) as it is indicated in Fig. 12. Therefore, a significant deviation of the transmitted (D_{PWM}) and received value of duty cycle (D_{rec}) occurs for $V_{IN\_sens} > 0.4$ V. Dependence of D_{PWM} and D_{rec} on V_{IN_sens} is shown in Fig. 12(a). The low values of the error of the duty cycle between the transmitted and received values (see Fig. 12(b)) indicate a very good mutual correspondence for values $D_{PWM/rec} >$ 40% (the error is not exceeding 11%). The time delay caused by the signal processing at the receiver side is shown in Fig. 13. The value of the delay fluctuates around 230 μs, which is insignificant for low-bitrate communication.

Signals transmitted and received in the time domain for selected values of V_{INsens} (−0.8 V, −0.4 V, 0 V and +0.4 V) are depicted in Fig. 14 to Fig. 17.

The results indicate that the frequency of the modulation signal f_{PWM} at the receiver side was precisely restored (f_{rec}

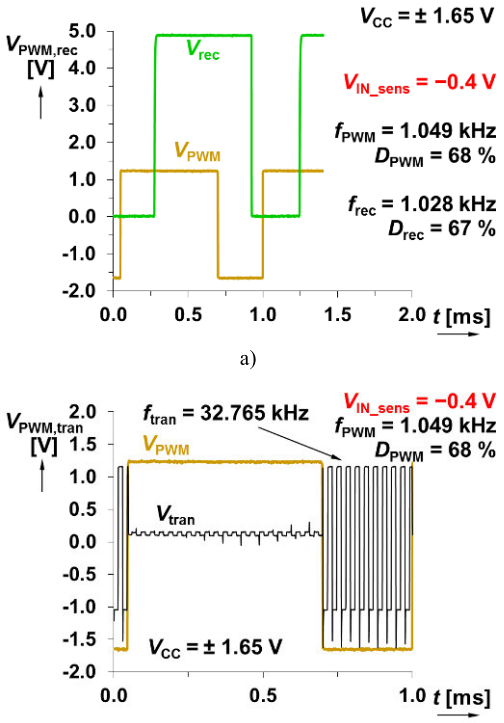

FIGURE 15. Transmission of DC voltage in the form of duty cycle for $V_{IN\_sens} = -0.4$ V (measurement): a) v_{PWM} and v_{rec}, b) v_{PWM} and v_{tran}.

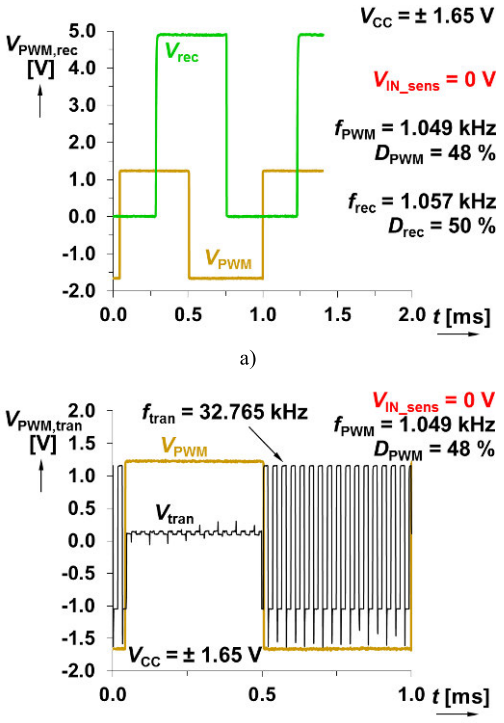

FIGURE 16. Transmission of DC voltage in the form of duty cycle for $V_{IN\_sens} = 0.0$ V (measurement): a) v_{PWM} and v_{rec}, b) v_{PWM} and v_{tran}.

also reaches the value of 1 kHz). The distance between the transmitter and the receiver was fixed to 20 cm in chosen measurement setup, which is sufficient for the transmission through a glass window of a plant aquarium. This distance can be extended up to several meters when different setting of the IR diode is chosen (increased supply voltage and current).

V. EXEMPLARY TEST OF THE WHOLE SYSTEM IN REAL ENVIRONMENT

The previous section focused on the general verification of the proposed concept, where V_{IN_sens} was supplied from a DC source in order to evaluate the performance of the system. However, usefulness of such a complex circuit should also be proven in practical use cases and in real environment. Transmission of information about illuminance from an aquarium for cultivation of exotic flowers, for instance plants [see Fig. 18 (a)], represents a perfect practical utilization of the proposed devices (transmitter and receiver). Sensor based on the photoresistor LDR5516 [21] was used. It was connected to the system in order to provide the V_{IN_sens} voltage dependent on the current value of the illuminance as shown in Fig. 18 (b). Here, the supply voltage of ±1.65 V was used. The lux-meter PU150 served for the measurement of the illuminance. The measurement was performed in the range from 30 lx up to 550 lx. The duty cycle D_{PWM} was varied by these values of illuminance in the range from 15% up to 90% while the received D_{rec} was sensed in range from 27% up to 88% (see Fig. 19(a)). The error between both curves (''dependence'' of transmitted and received duty cycles on illuminance), where

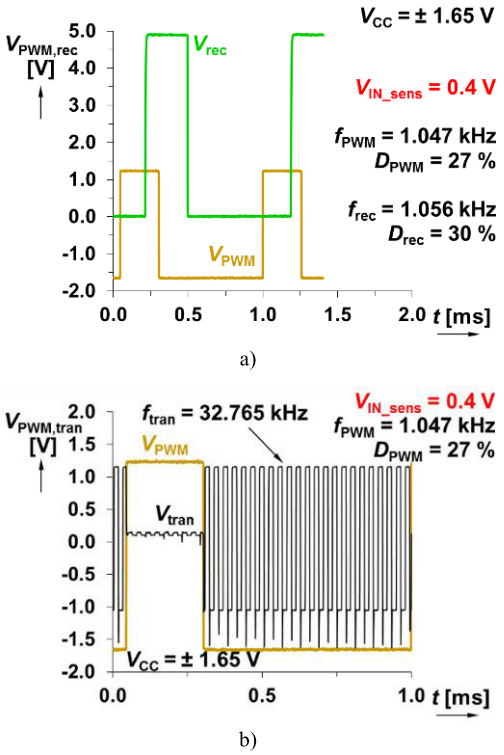

FIGURE 17. Transmission of DC voltage in the form of duty cycle for $V_{IN\_sens} = +0.4$ V (measurement): a) v_{PWM} and v_{rec}, b) v_{PWM} and v_{tran}.

D_{PWM} is the reference, is shown in Fig. 19(b). The results indicate D_{error} below 10% for illuminance higher than 40 lx. As it was already discussed, such an error is caused by the

TABLE 2. Comparison of the features of several application examples (transmission of information about physical quantity) in the field of General IR communication.

References	Purpose	Tested transmission distance (meters)	Sensed quantity	Transmitted parameter	Modulation technique	Software required	Prevailing character of the system	Demands on HW and SW (if required)	RF parts required	Active devices	Design area requirements
[23]	Control loop of motor drive	0.1	Speed (RPM)	DC voltage	PWM	Yes	Mixed	High	No	Commercial	High
[24]	Air conditioning	< 3	Temperature	Data	FSK, PWM, PPM	Yes	Digital	High	No	Commercial	Low
[25]	Medical applications	< 1	Respiratory rate, heartbeat	Time interval	ON-OFF keying	No	Mixed	High	Yes*	ASIC CMOS IC fabricated	Low
[26]	Counting and car profile visualization	N/A	ON/OFF state of point in matrix	Time distance of deactivated points	-	Yes	Digital	High	No	Commercial	High
This paper	Intensity of light measurement	0.2	Illuminance	Duty cycle	ON-OFF keying, PWM	No	Analog	Low	No	Universal purpose CMOS IC fabricated	Low

Notes: ASIC - Application Specific Integrated Circuit; FSK – frequency shift keying; PPM – pulse position modulation; PWM – pulse width modulation; RPM – revolutions per minute. *System based on ultra-wide-band techniques (UWB)

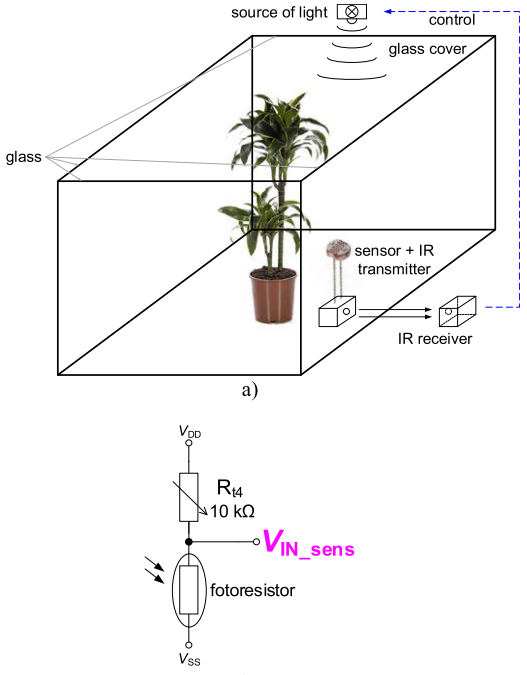

FIGURE 18. Example of application of the proposed system: a) transmission of measured data representing value of illuminance from aquarium box, b) sensor of illuminance based on a photoresistor.

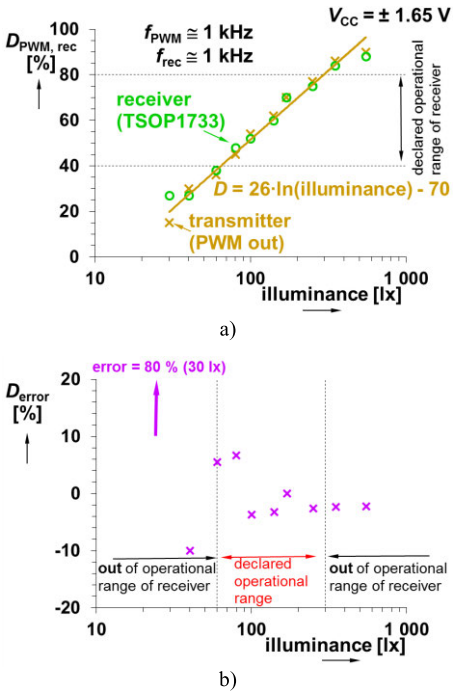

FIGURE 19. Measurement of illuminance using LDR5516 photoresistor-based readout as a source of V_{IN_sens} voltage: a) dependence of duty D_{PWM} and D_{rec} on illuminance, b) the error between the transmitted and received duty cycle.

limitation of the IR receiver [18] for low values of the duty cycle. The system can be extended with a regulation loop to control the light intensity, see Fig. 18(a), as a control branch from the receiver to the source of the light. It is not a part of this design.

VI. COMPARISON OF THE PROPOSED CONCEPT WITH SIMILAR APPLICATIONS UTILIZING IR TRANSMISSION

Special AEs are widely utilized for construction of building blocks used in complex communication systems as

TABLE 3. Comparison with the most similar concepts suitable for the same purposes as IR transmitter proposed in this paper.

References	Subject of transmission (sensed and transmitted quality)	Wavelength of modulated light during transmission	Direction of communication	Modulation type	Solution of modulation	Prevailing character of the system	Operable without software	Character of the system (area/topological complexity and processing)	Tested transmission distance	Number of HW parts (IC packages)	Power requirements (maximal used supply voltage / consumption)	Technology used for design of active devices	Suitable for low-cost application
[29]	Data	IR	Simplex	OFDM/PWM	HW/ SW	Mixed	No	Complex	N/A	[a]	N/A	BJT/ Commercial devices	Yes
[30]	Data	IR	Duplex	PWM	SW	Digital	No	Complex	10 m	2[b]	5V/-	Commercial devices	Yes
[31]	Data	VL + IR	Simplex	TDHM (PAM/PWM)	SW	Digital	No	Complex	N/A	[c]	-/[d]	N/A	No
[32]	Data	VL	Simplex/ Duplex	OFDM/PWM	SW	Mixed	No	Robust and Complex	2 m	[e]	14V/-	Commercial devices	No
[33]	Data	VL	Simplex/ Duplex	OFDM+ modifications	SW	Digital	No	Robust and Complex	2 m	[f]	N/A	FPGA, USRP, development board	No
This paper	Illuminance	IR	Simplex	PWM	HW	Analog	Yes	Simple	0.2 m	2(3)	3.3V/ 0.18 W	CMOS	Yes

Notes: N/A – information not available; BJT – bipolar junction transistor; CMOS – complementary metal oxide semiconductor transistor; VL – visible light, IR – infra red; PAM – pulse amplitude modulation; PWM – pulse width modulation; DSP – digital signal processor; TDHM – time domain hybrid modulation; OFDM – orthogonal frequency division multiplexing; FPGA – field programmable gate array; USRP - Universal Software Radio Peripheral

[a] – HW: DSP + PWM modulator (integrator + comparator + buffer + laser diode driver); clock > 5 GHz is required for DSP when PWM generated digitally
[b] – HW: microcontroller + USB/serial converter MAX232 (FTDI)
[c] – HW: is not clearly discussed, only the block concept is shown (> 8 blocks)
[d] – Only the total transmit power is shown (up to 14 W)
[e] – HW: very complex DSP/microprocessor (> 7 blocks)
[f] – HW: more than 6 (in the case of SW blocks even more)

shown in [22], for instance. The examples of practical applications (transmission of a physical quantity) of the IR communication-based systems are compared with newly proposed concept presented in this paper. However, application fields, where these systems are used, are different. Therefore, also different performances of these systems are required. The IR communication can be also useful as a way of non-galvanic feedback for power devices (motors working with PWM [23]), remote control systems for temperature and air conditioning purposes [24] or robust and highly reliable transmission of complex data from sensors (e.g. vital signs in medical applications) [25]. The IR concept serves beneficially also for security and counting purposes (gate/alarm) as well as for visualization of objects [26]. The general purpose and features of the designed system and the relevant examples in selected application fields are compared in Table 2. Note that the IR communication can be used for indoor communication [27], [28] with various sophisticated modulations and processing techniques (see [27]).

Five solutions were identified in literature which can (after certain modifications) use IR or visible light spectrum for remote/wireless communication for the same purpose as proposed in this paper (measurement of illuminance and short-range transmission of the information).

Their comparison is presented in Table 3. One of the main differences between the designed concept and the other designs is in the complexity. The other identified solutions require a digital part, a clock, and/or several different levels of voltage supply for the tasks similar to our use case. Studied IR transmitter operates with a single supply voltage. The measurement of illuminance and data transmission with systems presented in [29]–[33] also requires an analog to digital converter (ADC) block. This requirement brings additional discrete device or block in the form of DSP, FPGA chip, or similar.

The designed solution does not use an ADC in the transmitter front-end as well as digital-to-analog conversion (DAC) in the receiver neither any special and complex modulation technique. Moreover, compared to [29]–[33], additional software is not necessary. Therefore, costs are as low as possible. There are interesting systems for IR communication using PWM or similar advanced methods. However, their HW [29], [33] or SW [31]–[33] complexity is higher than in case of analog concept presented in this paper. Next, they

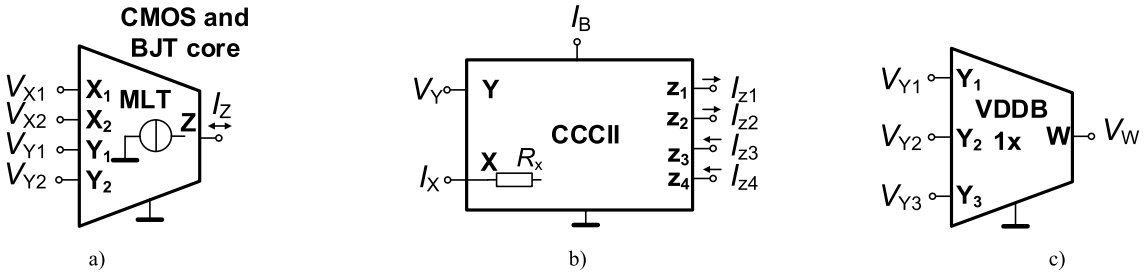

FIGURE A. Schematic symbols of active elements (AEs) used in the designed transmitter: a) multiplier with current output terminal (CMOS and BJT core), b) current controlled current conveyor of second generation (CCCII), c) voltage differencing difference buffer (VDDB).

are optimized for other purposes (general data transmission) than the designed IR communication system. The trade-off between the performance and the effectivity is not very good in these cases. Beside the solutions with large operating distances [30], [32], [33], the concepts most suitable for studied purpose [29], [31] have significant drawbacks: a high number of used IC packages [29], necessity of a digital part and SW programming [29], [30] and a high number of functional SW blocks (requirements on the HW performance of the digital system) [31]–[33]. Consequently, the designed solution fits very well the intended purposes (direct measurement and transmission of illuminance and low power consumption) and signal transmission over short distances.

VII. CONCLUSION

In this paper, novel concept of IR remote transmission system using PWM and ON/OFF keying was presented. The system is designed to process either slowly changing signals or data with low bitrate. The whole system is analog only. The majority of active elements required for the proposed concept was realized using AEs developed recently in I3T 0.35 μm CMOS process [16]. The input information (voltage) is processed and transferred in the form of the duty cycle change, which is the key feature of the used IR PCM remote receiver. The designed transmitter (see Fig. 1) is capable of duty cycle variation from 7% up to 83%. Off-the-shelf IR receiver is declared to sense properly the duty cycle between 40% and 80% (see Fig. 9 in [18]), which is sufficient for the designed application.

Nevertheless, performed laboratory experiments detected the usable range between 27% and 82%. For the most significant part of the considered operational range, the error between the received and transmitted duty cycles reaches maximally 11%. The sensing of illuminance represents one practical application of the proposed concept. The photoresistor-based readout served as the source of input data for the transmitter. Measurement of illuminance was tested for values from 30 lx to 550 lx.

The transmitter provided a waveform with the duty cycle between 15% and 90% whereas; receiver evaluated the duty cycle in the range from 27% to 88%. The error between the transmitted and received values in the declared range of operation (between 40% and 80% duty cycle of the IR receiver) is less than 10%. The power consumption of the TSOP1733 IR receiver reaches 50 mW (5 V, 10 mA). The power consumption of the whole transmitter (including the IR diode) reaches approximately 150 mW (average), maximally 180 mW in the case of using the illuminance sensor. Laboratory tests confirmed expected features as well as applicability of the proposed device.

Compact IR transmitter for agriculture and vegetation applications was designed that can be also used for other low-cost and low-speed use cases. Its functionality was verified by several experimental measurements. The main contributions of the designed concept are as follows:

1) When compared with more complex solutions requiring digital parts [29]–[33], a very simple analog solution for transmission of analog quantity as well as low-bitrate data transfer in the form of the duty cycle variation driving IR LED was proposed and realized,
2) In comparison with discrete analog solutions (see Table 1), proposed concept simplifies the construction of the IR transmitter. Thanks to CMOS integrated building blocks developed recently [16], the number of discrete IC packages is reduced,
3) Unlike the standard way of design with commercially available active devices as well as digital-based solutions (DSP, FPGA, microcontrollers), the presented concept, in the case of serial fabrication of the transmitter (single IC), reduces cost and also power consumption, when operating.
4) The proposed IR communication system needs no additional analog-to-digital conversion – analog signal from the photoresistor is processed directly.

The presented concept is operational and based on well-known active parts. However, the design is novel in the usage of specific building blocks, in selected topologies, and their mutual interconnection. To the best of authors' knowledge, a similarly working analog system using easily integrable analog blocks for illuminance sensing and wireless optic transmission has not been reported so far.

APPENDIX

(Please see Fig. A) The proposed IR transmitter uses developed active elements available as AEs integrated on chip (single package) in 0.35 μm ON Semiconductor CMOS process I3T25 (3.3 V) [16]. Each package includes a multiplier (MLT) in CMOS and BJT version abbreviated as CMOS

MLT and BJT MLT (Fig. A(a)). Both devices have identical transfer function: $I_Z = (V_{X1} - V_{X2}) \cdot (V_{Y1} - V_{Y2}) \cdot k$. The most important difference for the processed signals and considered frequency range, used in this work, is the value of the transconductance constant ($k \cong 1.3$ mA/V^2 for CMOS version and $k \cong 4.9$ mA/V^2 for BJT type) [16].

The behavior of current controlled current conveyor of second generation (CCCII) is defined by: $I_Y = 0$, $V_X = V_Y + R_X I_X$, where I_X is the current flowing through X terminal and $I_{Z4} = I_{Z3} = -I_{Z2} = -I_{Z1} = I_X$. Note that the unused current outputs are grounded directly. The input resistance R_X can be adjusted by the bias I_B current in accordance with the relation: $R_X = 20 \cdot I_B^{-0.8}$. The value of R_X can be adjusted between low hundreds and thousands of Ohms [16]. The voltage differencing difference buffer (VDDB) serves for addition and subtraction of voltages: $V_W = V_{Y1} - V_{Y2} + V_{Y3}$ and offers a low impedance W output [16].

REFERENCES

[1] Y. Lee and J. P. Choi, "Performance evaluation of high-frequency mobile satellite communications," *IEEE Access*, vol. 7, pp. 49077–49087, 2019, doi: 10.1109/access.2019.2909885.
[2] J. W. Leis, *Wired, Wireless, and Optical Systems, Communication Systems Principles Using MATLAB*, 1st ed. Hoboken, NJ, USA: Wiley, 2019, pp. 37–154.
[3] S. Zvanovec, P. Chvojka, P. A. Haigh, and Z. Ghassemlooy, "Visible light communications towards 5G," *Radioengineering*, vol. 24, no. 1, pp. 1–9, Apr. 2015, doi: 10.13164/re.2015.0001.
[4] H. Santos, C. Sturm, and J. Ponte, *Radio Systems Engineering: A Tutorial Approach*, 1st ed. Cham, Switzerland: Springer, 2015, p. 253.
[5] D. Han, J. Lee, J. Im, S. Sim, S. Lee, and H. Han, "A novel framework of detecting convective initiation combining automated sampling, machine learning, and repeated model tuning from geostationary satellite data," *Remote Sens.*, vol. 11, no. 12, p. 1454, Jun. 2019, doi: 10.3390/rs11121454.
[6] N. Xia, L. Cheng, and M. Li, "Mapping urban areas using a combination of remote sensing and geolocation data," *Remote Sens.*, vol. 11, no. 12, p. 1470, Jun. 2019, doi: 10.3390/rs11121470.
[7] D. Vansteenwegen, K. Ruddick, A. Cattrijsse, Q. Vanhellemont, and M. Beck, "The pan-and-tilt hyperspectral radiometer system (PANTHYR) for autonomous satellite validation measurements-prototype design and testing," *Remote Sens.*, vol. 11, no. 11, pp. 1–21, Jun. 2019, doi: 10.3390/rs11111360.
[8] J. M. Kahn and J. R. Barry, "Wireless infrared communication," *Proc. IEEE*, vol. 85, no. 2, pp. 265–298, Feb. 1997, doi: 10.1109/5.554222.
[9] Z. Ghassemlooy, A. R. Hayes, N. L. Seed, and E. D. Kaluarachchi, "Digital pulse interval modulation for optical communications," *IEEE Commun. Mag.*, vol. 36, no. 12, pp. 95–99, Dec. 1998, doi: 10.1109/35.735885.
[10] W. N. Waggener, *Pulse Code Modulation Systems Design*. Norwood, MA, USA: Artech House, 1998, p. 329.
[11] Z. Ghassemlooy and A. R. Hayes, "Digital pulse interval modulation for IR communication systems—A review," *Int. J. Commun. Syst.*, vol. 13, nos. 7–8, pp. 519–536, Dec. 2000, doi: 10.1002/1099-1131(200011/12)13:7/8<519::AID-DAC454>3.0.CO;2-5.
[12] S. Guo, K.-H. Park, and M.-S. Alouini, "Ordered sequence detection and barrier signal design for digital pulse interval modulation in optical wireless communications," *IEEE Trans. Commun.*, vol. 67, no. 4, pp. 2880–2892, Apr. 2019, doi: 10.1109/tcomm.2018.2890249.
[13] D. Dinh, V. A. Truong, A. N.-P. Tran, H. X. Le, and H. T.-T. Pham, "Non-invasive glucose monitoring system utilizing near-infrared technology," in *Proc. 7th Int. Conf. Develop. Biomed. Eng. Vietnam (BME)*, Jun. 2018, pp. 401–405, doi: 10.1007/978-981-13-5859-3_71.
[14] S. Preto and C. C. Gomes, "Lighting in the workplace: Recommended illuminance (LUX) at workplace environs," in *Proc. Int. Conf. Appl. Hum. Factors Ergonom. (AHFE), Adv. Design Inclusion*, Jun. 2018, pp. 180–191, doi: 10.1007/978-3-319-94622-1_18.
[15] M. Doane and E. Harding, *How to Raise a Plant: And Make it Love You Back*. London, U.K.: Laurence King Publishing, 2018, p. 112.
[16] R. Sotner, J. Jerabek, L. Polak, R. Prokop, and V. Kledrowetz, "Integrated building cells for a simple modular design of electronic circuits with reduced external complexity: Performance, active element assembly, and an application example," *Electronics*, vol. 8, no. 5, p. 568, May 2019, doi: 10.3390/electronics8050568.
[17] Vishay Semiconductors. *High Power Infrared Emitting Diode, 940 nm, GaAlAs, MQW TSAL6100*. Accessed: Nov. 25, 2019. [Online]. Available: https://www.vishay.com/docs/81009/tsal6100.pdf
[18] Vishay Telefunken. *Photo Modules for PCM Remote Control Systems TSOP1733*. Accessed: Nov. 25, 2019. [Online]. Available: http://www.farnell.com/datasheets/1804482.pdf
[19] W. S. Chung, H. Kim, H.-W. Cha, and H.-J. Kim, "Triangular/square-wave generator with independently controllable frequency and amplitude," *IEEE Trans. Instrum. Meas.*, vol. 54, no. 1, pp. 105–109, Feb. 2005, doi: 10.1109/TIM.2004.840238.
[20] ON Semiconductor. *Amplifier Transistors PNP Silicon BC557*. Accessed: Nov. 25, 2019. [Online]. Available: https://www.onsemi.com/pub/Collateral/BC556B-D.PDF
[21] Token. *CDS Photoresistors PGM/LDR5516*. Accessed: Nov. 25, 2019. [Online]. Available: https://www.tme.eu/Document/0b7aec6d26675b47f9e54d893cd4521b/PGM5506.pdf
[22] A. K. AboulSeoud, M. H. Aly, and N. Azzam, "A CCII-amplifier for high-gain and high bandwidth outdoor WOC applications," in *Proc. 5th Int. Conf. Saudi Tech. Conf. (STCEX)*, Jun. 2009, pp. 1–8.
[23] I. R. Agung, S. Huda, and I. W. A. Wijaya, "Speed control for DC motor with pulse width modulation (PWM) method using infrared remote control based on ATmega16 microcontroller," in *Proc. Int. Conf. Smart Green Technol. Electr. Inf. Syst. (ICSGTEIS)*, Nov. 2014, pp. 108–112, doi: 10.1109/ICSGTEIS.2014.7038740.
[24] Y. Ren and, "The remote infrared remote control system based on LPC1114," in *Proc. AIP Conf.*, May 2018, vol. 1967, no. 1, pp. 030044-1–030044-7, doi: 10.1063/1.5039072.
[25] Z. Zhang, Y. Li, K. Mouthaan, and Y. Lian, "A miniature mode reconfigurable inductorless IR-UWB transmitter–receiver for wireless short-range communication and vital-sign sensing," *IEEE J. Emerg. Sel. Topics Circuits Syst.*, vol. 8, no. 2, pp. 294–305, Jan. 2018, doi: 10.1109/JETCAS.2018.2799930.
[26] H. S. Katri and S. B. Somani, "Infrared-based system for vehicle counting and classification," in *Proc. Int. Conf. Pervas. Comput. (ICPC)*, Jan. 2015, pp. 1–5, doi: 10.1109/PERVASIVE.2015.7086998.
[27] X. You, J. Chen, and C. Yu, "Efficient indoor data transmission with full dimming control in hybrid visible light/infrared communication systems," *IEEE Access*, vol. 6, pp. 77675–77684, 2018, doi: 10.1109/access.2018.2883750.
[28] D. Karunatilaka, F. Zafar, V. Kalavally, and R. Parthiban, "LED based indoor visible light communications: State of the art," *IEEE Commun. Surveys Tuts.*, vol. 17, no. 3, pp. 1649–1678, 3rd Quart., 2015, doi: 10.1109/comst.2015.2417576.
[29] M. Koyuncu, C. Bos, and W. A. Serdijn, "A PWM modulator for wireless infrared communication," in *Proc. Int. Workshop Semiconductors, Circuits, Syst. Signal Process.*, Nov. 2000, pp. 1–4.
[30] A. Shahriar, M. Chakraborty, S. Hossain, D. Halder, and N. B. Chowdhury, "Wireless infrared communication between two computers by MATLAB," in *Proc. Int. Forum Strategic Technol. (IFOST)*, Oct. 2014, pp. 60–64, doi: 10.1109/IFOST.2014.6991072.
[31] X. You, J. Chen, Y. Zhong, S. Chen, and C. Yu, "Efficient dimming control with time domain hybrid modulation in indoor hybrid visible light/infrared communication systems," in *Proc. Int. Conf. Photon. Switching Comput. (PSC)*, Jul. 2019, pp. 1–3, doi: 10.23919/PS.2019.8817648.
[32] T. Adiono, A. Pradana, R. V. W. Putra, W. A. Cahyadi, and Y. H. Chung, "Physical layer design with analog front end for bidirectional DCO-OFDM visible light communications," *Optik*, vol. 138, pp. 103–118, Jun. 2017, doi: 10.1016/j.ijleo.2017.03.046.
[33] S. Vappangi and V. Mani, "Concurrent illumination and communication: A survey on Visible Light Communication," *Physical Commun.*, vol. 33, pp. 90–114, Apr. 2019, doi: 10.1016/j.phycom.2018.12.017.

ROMAN SOTNER was born in Znojmo, Czech Republic, in 1983. He received the M.Sc. and Ph.D. degrees from the Brno University of Technology, Czech Republic, in 2008 and 2012, respectively. He is currently an Associate Professor with the Department of Radio Electronics, Faculty of Electrical Engineering and Communication, Brno University of Technology. His interests are analog circuits (active filters, oscillators, audio, etc.), circuits in the current mode, circuits with direct electronic controlling possibilities, especially, and computer simulation.

JAN JERABEK was born in Bruntal, Czech Republic, in 1982. He received the B.Sc. and M.Sc. degrees, and the Ph.D. degree in electrical engineering from the Brno University of Technology, Czech Republic, in 2005, 2007, and 2011, respectively. He is currently an Associate Professor with the Department of Telecommunications, Faculty of Electrical Engineering and Communication, Brno University of Technology. His researches focus on analogue signal processing, including circuit design, analyses, and measurements.

LADISLAV POLAK (Member, IEEE) was born in Štúrovo, Slovakia, in 1984. He received the M.Sc. and Ph.D. degrees in electronics and communication from the Brno University of Technology (BUT), Czech Republic, in 2009 and 2013, respectively. He is currently an Associate Professor with the Department of Radio Electronic (DREL), BUT. His research interests are wireless communication systems, RF measurement, signal processing, and computer-aided analysis.

JIRI PETRZELA was born in Brno, Czech Republic, in 1978. He received the M.Sc. and Ph.D. degrees in the field of the theoretical electronics in 2003 and 2007, respectively. He is currently working as an Associate Professor with the Department of Radio Electronics, Faculty of Electrical Engineering and Communications, Brno University of Technology, Czech Republic. His research interests include numerical methods in electrical engineering, nonlinear dynamics, chaos theory, analog lumped circuit design, and computer-aided analysis.

WINAI JAIKLA was born in Buriram, Thailand. He received the B.S.I.Ed. degree in telecommunication engineering from the King Mongkut's Institute of Technology Ladkrabang (KMITL), Thailand, in 2002, the M.Tech.Ed. degree in electrical technology, and the Ph.D. degree in electrical education from the King Mongkut's University of Technology North Bangkok (KMUTNB) in 2004 and 2010, respectively. His research interests include electronic communications, analog signal processing, and analog integrated circuits.

SUNTI TUNTRAKOOL received the B.S. degree in industrial education in telecommunication engineering major from the King Mongkut's Institute of Technology Ladkrabang, Ladkrabang, Bangkok, Thailand, in 1993, and the M.S. degree in electrical engineering from Vanderbilt University, Nashville, TN, USA, in 2004. His research interests include digital signal processing, biomedical signal processing, mouse renal sympathetic nerve activity, and autonomic control of the cardiovascular systems.